Hindawi
Advances in Materials Science and Engineering
Volume 2022, Article ID 5314863, 11 pages
https://doi.org/10.1155/2022/5314863

Research Article

Effect of Mold Flux Containing Ce_2O_3 on the Contents of Aluminum, Silicon, and Titanium in Incoloy825 Super Alloy

Geng Xin,[1,2] Boyang Li,[1] Zhouhua Jiang ,[1,2] and Hou Yu[1]

[1]*School of Metallurgy, Northeastern University, Shenyang 110819, China*
[2]*State Key Laboratory of Rolling and Automation, Northeastern University, Shenyang 110819, China*

Correspondence should be addressed to Zhouhua Jiang; jiangzh@smm.neu.edu.cn

Received 1 June 2022; Accepted 29 August 2022; Published 11 October 2022

Academic Editor: Alicia E. Ares

The effect of mold flux containing Ce_2O_3 on the contents of aluminum, silicon, and titanium in Incoloy825 super alloy was investigated based on the slag-steel interfacial chemical reaction experiment between mold flux and alloy. Firstly, the activity model of the $CaO\text{-}SiO_2\text{-}Al_2O_3\text{-}Na_2O\text{-}MgO\text{-}CaF_2\text{-}Ce_2O_3$ slag system was established according to the ion and molecule coexistence theory (IMCT), and the calculation results show that with the increase of Ce_2O_3 content in the mold flux, the activity of Al_2O_3 decreases significantly and the activity of SiO_2 decreases and gradually tends to 0. Secondly, thermodynamic calculations of the slag-steel interfacial chemical reaction revealed that the main chemical reaction in this study system is $[Ti] + (SiO_2) = [Si] + (TiO_2)$. With the increase of Ce_2O_3 content in the mold flux, the slag-steel interfacial chemical reaction is weakened and the oxidation of Al and Ti in steel is inhibited. Finally, the results of slag-steel reaction experiment show that the increase rate of Al content increases from 1.03% to 10.31%, the increase rate of Si content decreases from 55.95% to 31.25%, and the oxidation rate of Ti content decreases from 33.27% to 20.00% when Ce_2O_3 content in the mold flux increases from 0% to 15% and the slag-steel reaction for 40 mins.

1. Introduction

Incoloy825 super alloy is a fully austenitic nickel-based alloy treated by Ti stabilization, which has good resistance to stress corrosion cracking, crevice corrosion, and pitting corrosion [1–3]. Therefore, Incoloy825 is used in corrosion-resistant and extremely hot environments, such as heat exchanger, turbine engine, turbine, nuclear power reactor core, and other important components [4–6].

At present, Incoloy825 is mainly smelted using the electroslag remelting (ESR) [7, 8], while it is difficult to use continuous casting for large-scale production. In general, the composition of the commonly used continuous casting mold flux is shown in Figure 1 in region A, its high content of SiO_2 is prone to interfacial chemical reactions with the high content of Ti and Al in Incoloy825, as shown in (1). The reaction not only causes oxidation loss of Ti and Al but also leads to changes in the properties of the mold flux, which affects the continuous casting process [9–12].

$$2[\mathrm{M}] + x(\mathrm{SiO_2}) = x[\mathrm{Si}] + 2(\mathrm{MO}_x). \tag{1}$$

In order to solve the abovementioned problems, researchers have proposed the use of low-reactive $CaO\text{-}Al_2O_3$-based mold fluxes with $SiO_2 \leq 10$ wt% (as shown in region B in Figure 1) for steel grades with serious slag-steel reaction [13–16]. However, the high activity of CaO in the mold fluxes tends to generate high melting point $CaTiO_3$ with TiO_2, as shown in Eq. (2). The high melting point minerals will enhance the crystallization ability of the mold flux and affect the penetration of liquid slag into the gap between mold and primary billet shell, resulting in insufficient lubrication ability of the mold flux [17–19]. Therefore, Piao et al. reduced the crystallization temperature and critical cooling rate by adding BaO to the mold flux [20]. But, the liquidus temperature of Incoloy825 is 1646 K which is much lower than that of steel (1803 K), so this slag system is not suitable for Incoloy825 continuous casting production.

$$(\mathrm{CaO}) + (\mathrm{TiO_2}) = (\mathrm{CaTiO_3}). \tag{2}$$

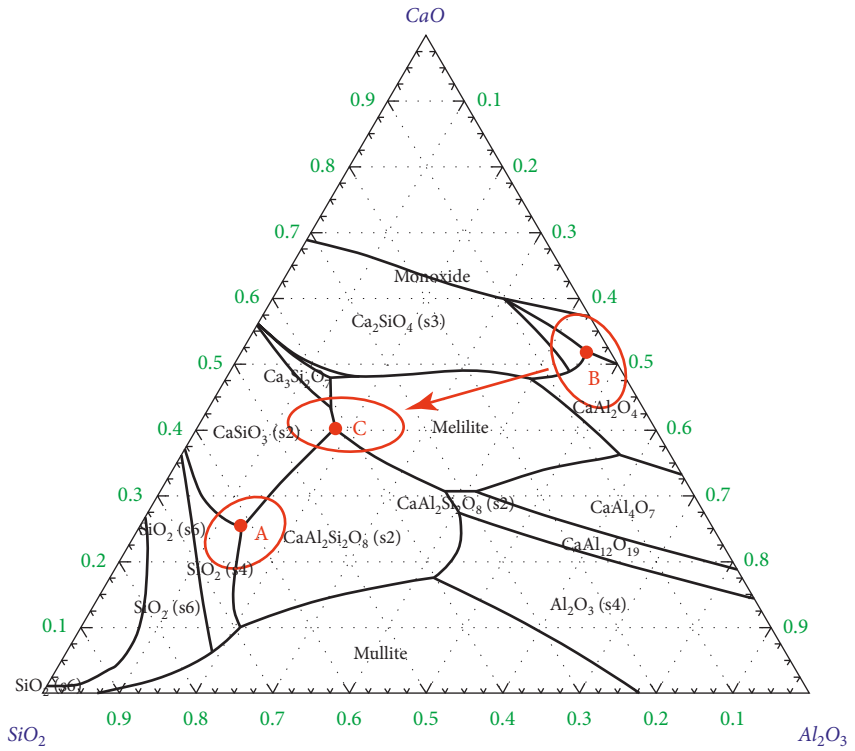

Figure 1: Phase diagram of CaO-SiO_2-Al_2O_3.

Aiming at the oxidation loss of Ti and Al in Incoloy825 and the lubrication problem in continuous casting process, a new type of mold flux based on region C in Figure 1 of CaO-SiO_2-Al_2O_3-based mold flux was developed in this paper. The main precipitated phases in this region are melilite, $CaAl_2Si_2O_8$, and $CaSiO_3$, so the activity of Al_2O_3 and SiO_2 is low and the slag-steel interfacial chemical reaction is weak, which can control the oxidation loss of group elements in the steel. At the same time, the content of SiO_2 in mold flux is high, which can ensure the lubricating performance of the mold flux.

In order to further prevent the oxidation loss of Ti in steel, TiO_2 is often added to the mold flux [21–24]. However, when TiO_2 is added into the CaO-SiO_2-Al_2O_3 system, $CaSiO_3$ will be transformed into $CaTiO_3$ [25, 26], as shown in Eq. (3), which will result in low effective activity of TiO_2 and increased activity of SiO_2. In addition, the lower temperature of the continuous casting process will result in the preferential precipitation of $CaTiO_3$, which has a higher melting point, and this will affect the lubricating ability of the casting agent. As a result, the addition of TiO_2 does not work as well as it should.

$$(CaSiO_3) + (TiO_2) = (CaTiO_3) + (SiO_2). \tag{3}$$

This paper innovatively proposes to add Ce_2O_3 to the mold flux to form $Ce_2Si_2O_7$ [27] and $CeAlO_3$ [28], which can effectively reduce the activity of Al_2O_3 and SiO_2 and inhibit the chemical reaction at the slag-steel interface. In addition, the melting point of the main compound $Ce_2Si_2O_7$ (2043 K) [27] is 200 K lower than that of $CaTiO_3$ (2243 K) [26], which ensures the lubrication performance of mold flux. The research results will provide theoretical basis for low activity mold flux and have important theoretical significance for developing Incoloy825 continuous casting mold flux.

2. Thermodynamic Calculation of Slag-Steel Reaction

2.1. Activity Calculation of Elements in Steel and Components in Slag. As previously described, the equations for slag-steel interfacial chemical reaction of Ti and Al in Incoloy825 with CaO-SiO_2-Al_2O_3-based mold flux are shown in Eq. (4), Eq. (6), and Eq. (8).

$$[Ti] + SiO_2 = [Si] + TiO_2. \tag{4}$$

$$\begin{aligned} \Delta G_1^\theta &= -3446.49 - 26.04T, \\ \Delta G_1 &= \Delta G_1^\theta + RT\ln K_1 = \Delta G_1^\theta + RT\ln\frac{a_{Si}\cdot a_{TiO_2}}{a_{Ti}\cdot a_{SiO_2}} \\ &= \Delta G_1^\theta + RT\ln\frac{f_{Si}\cdot w[Si]_{\%}}{f_{Ti}\cdot w[Ti]_{\%}} + RT\ln\frac{a_{TiO_2}}{a_{SiO_2}}, \end{aligned} \tag{5}$$

$$4[Al] + 3(SiO_2) = 3[Si] + 2(Al_2O_3), \tag{6}$$

$$\begin{aligned} \Delta G_2^\theta &= -686233.57 + 112.20T, \\ \Delta G_2 &= \Delta G_2^\theta + RT\ln K_2 = \Delta G_2^\theta + RT\ln\frac{a_{Si}^3\cdot a_{Al_2O_3}^2}{a_{Al}^4\cdot a_{SiO_2}^3} \\ &= \Delta G_2^\theta + RT\ln\frac{f_{Si}^3\cdot w[Si]_{\%}^3}{f_{Al}^4\cdot w[Al]_{\%}^4} + RT\ln\frac{a_{Al_2O_3}^2}{a_{SiO_2}^3}. \end{aligned} \tag{7}$$

$$3[\mathrm{Ti}] + 2(\mathrm{Al_2O_3}) = 4[\mathrm{Al}] + 3(\mathrm{TiO_2}), \tag{8}$$

$$\begin{aligned}\Delta G_3^{\theta} &= 675894.11 - 190.32T,\\ \Delta G_3 = \Delta G_3^{\theta} + RT\ln K_3 &= \Delta G_3^{\theta} + RT\ln\frac{a_{\mathrm{Al}}^4 \cdot a_{\mathrm{TiO_2}}^3}{a_{\mathrm{Ti}}^3 \cdot a_{\mathrm{Al_2O_3}}^2}\\ &\&9; = \Delta G_3^{\theta} + RT\ln\frac{f_{\mathrm{Al}}^4 \cdot w[\mathrm{Al}]_{\%}^4}{f_{\mathrm{Ti}}^3 \cdot w[\mathrm{Ti}]_{\%}^3} + RT\ln\frac{a_{\mathrm{TiO_2}}^3}{a_{\mathrm{Al_2O_3}}^2},\end{aligned} \tag{9}$$

where ΔG is the reaction Gibbs free energy, $\Delta G^{\theta}$is the standard reaction Gibbs free energy, K is the reaction equilibrium constant, $a_{\mathrm{Al_2O_3}}$, $a_{\mathrm{SiO_2}}$, and $a_{\mathrm{TiO_2}}$ are the activities of Al_2O_3, SiO_2, and TiO_2 in slag, f_{Al}, f_{Si}, and f_{Ti} are the activity coefficients of Al, Si, and Ti in steel, which can be calculated by Eq. (10), respectively, and the activity interaction coefficients are listed in Table 1.

$$\lg f_i = \sum\left(e_i^j w[\%j]\right). \tag{10}$$

According to the composition of Incoloy825 (Table 2) and equation (10), the activity coefficients and activity of components in steel can be calculated as, $f_{\mathrm{Al}} = 0.205$, $a_{\mathrm{Al}} = 0.020$, $f_{\mathrm{Si}} = 0.144$, $a_{\mathrm{Si}} = 0.048$, $f_{\mathrm{Ti}} = 0.746$, and $a_{\mathrm{Ti}} = 0.753$. The calculations show that a_{Ti} is much greater than a_{Al}, suggesting that Ti is more susceptible to oxidation than Al.

In order to better understand the role of Ce_2O_3 in mold flux, $a_{\mathrm{Al_2O_3}}$ and $a_{\mathrm{SiO_2}}$ of S0~S4 (Table 3) are calculated according to IMCT [34, 35]. On the basis of IMCT, the mole fraction of each oxide could be assigned as $b_1 = n^o_{\mathrm{CaO}}$, $b_2 = n^o_{\mathrm{SiO_2}}$, $b_3 = n^o_{\mathrm{Al_2O_3}}$, $b_4 = n^o_{\mathrm{Na_2O}}$, $b_5 = n^o_{\mathrm{MgO}}$, $b_6 = n^o_{\mathrm{CaF_2}}$, and $b_7 = n^o_{\mathrm{Ce_2O_3}}$ to represent the chemical composition of the slag, and each of n_i^ocould be expressed by (11). The relevant compounds and chemical reactions of the present slag are listed in Tables 4 and 5, respectively. The composition of mold fluxes is shown in Table 3.

$$n_i^o = \frac{n_i}{\sum n_i}. \tag{11}$$

According to the description of IMCT, the formulas for calculating the activity of (12) components are established as follows:

$$\begin{aligned}
&N_{\mathrm{S1}} + N_{\mathrm{S2}} + \ldots + N_{\mathrm{C40}} = \sum N_i = 1,\\
&b_1 = (1/2N_{\mathrm{S1}} + N_{\mathrm{C1}} + 2N_{\mathrm{C2}} + 3N_{\mathrm{C3}} + N_{\mathrm{C5}} + N_{\mathrm{C6}} + N_{\mathrm{C7}} + 3N_{\mathrm{C8}} + 12N_{\mathrm{C9}} + N_{\mathrm{C22}} + 2N_{\mathrm{C23}} + N_{\mathrm{C24}} + N_{\mathrm{C25}}\\
&\quad + N_{\mathrm{C26}} + 3N_{\mathrm{C27}} + N_{\mathrm{C28}} + N_{\mathrm{C29}} + 2N_{\mathrm{C30}} + 3N_{\mathrm{C31}} + 3N_{\mathrm{C32}} + 3N_{\mathrm{C33}} + 11N_{\mathrm{C34}})\sum n_i,\\
&b_2 = (N_{\mathrm{S2}} + N_{\mathrm{C1}} + N_{\mathrm{C2}} + N_{\mathrm{C3}} + 2N_{\mathrm{C4}} + 2N_{\mathrm{C10}} + N_{\mathrm{C11}} + 2N_{\mathrm{C12}} + N_{\mathrm{C13}} + N_{\mathrm{C14}} + N_{\mathrm{C15}} + 2N_{\mathrm{C22}} + 2N_{\mathrm{C23}}\\
&\quad + 3N_{\mathrm{C24}} + 5N_{\mathrm{C25}} + 3N_{\mathrm{C26}} + 6N_{\mathrm{C27}} + N_{\mathrm{C28}} + 2N_{\mathrm{C29}} + 2N_{\mathrm{C30}} + 2N_{\mathrm{C31}} + 2N_{\mathrm{C32}} + 2N_{\mathrm{C35}} + 4N_{\mathrm{C36}}\\
&\quad + 6N_{\mathrm{C37}} + 5N_{\mathrm{C38}} + 2N_{\mathrm{C39}} + 6N_{\mathrm{C40}})\sum n_i,\\
&b_3 = (N_{\mathrm{S3}} + N_{\mathrm{C5}} + 2N_{\mathrm{C6}} + 6N_{\mathrm{C7}} + N_{\mathrm{C8}} + 7N_{\mathrm{C9}} + 3N_{\mathrm{C10}} + N_{\mathrm{C16}} + 3N_{\mathrm{C17}} + 9N_{\mathrm{C18}} + N_{\mathrm{C19}} + N_{\mathrm{C20}} + 11N_{\mathrm{C21}}\\
&\quad + N_{\mathrm{C22}} + N_{\mathrm{C23}} + 2N_{\mathrm{C24}} + 3N_{\mathrm{C33}} + 7N_{\mathrm{C34}} + N_{\mathrm{C35}} + N_{\mathrm{C36}} + N_{\mathrm{C37}} + 2N_{\mathrm{C38}})\sum n_i,\\
&b_4 = \frac{1}{3}N_{\mathrm{S4}} + N_{\mathrm{C11}} + N_{\mathrm{C12}} + N_{\mathrm{C13}} + N_{\mathrm{C16}} + N_{\mathrm{C17}} + N_{\mathrm{C18}} + N_{\mathrm{C25}} + N_{\mathrm{C26}} + N_{\mathrm{C27}} + N_{\mathrm{C35}} + N_{\mathrm{C36}} + N_{\mathrm{C37}}\\
&\quad + 2N_{\mathrm{C38}} + N_{\mathrm{C39}} + 6N_{\mathrm{C40}})\sum n_i,\\
&b_5 = \left(\frac{1}{2}N_{\mathrm{S5}} + N_{\mathrm{C14}} + N_{\mathrm{C15}} + N_{\mathrm{C19}} + N_{\mathrm{C28}} + N_{\mathrm{C29}} + N_{\mathrm{C30}} + N_{\mathrm{C31}} + N_{\mathrm{C39}} + 2N_{\mathrm{C40}}\right)\sum n_{i,}\\
&b_6 = \left(\frac{1}{3}N_{\mathrm{S6}} + N_{\mathrm{C32}} + N_{\mathrm{C33}} + N_{\mathrm{C34}}\right)\sum n_i,\\
&b_7 = \left(\frac{1}{7}N_{\mathrm{S7}} + N_{\mathrm{C20}} + N_{\mathrm{C21}}\right)\sum n_i.
\end{aligned} \tag{12}$$

The system of nonlinear equations from (12) is solved using MATLAB software, which allows the solution of N_{S1} to N_{S7}, that is, solving for the concentration of the action of each group element.

The addition of Ce_2O_3 to the mold flux has an important effect on $a_{\mathrm{Al_2O_3}}$ and $a_{\mathrm{SiO_2}}$ as shown in Figure 2. With the increase of Ce_2O_3 content in mold flux, $a_{\mathrm{Al_2O_3}}$ decreases significantly and $a_{\mathrm{SiO_2}}$ decreases and gradually tends to 0,

Table 1: Activity interaction coefficient e_i^j of the constituent in the present work.

e_i^j	Al	Cr	Cu	Mn	Mo	Ni	Si	Ti
Al	0.040 [29]	0.045 [29]		0.034 [29]		-0.0376 [30]		
Si	0.058 [30]	−0.021 [31]				−0.009 [32]	0.132 [29]	
Ti		0.025 [33]	0.014 [33]	−0.12 [33]	0.016 [33]	−0.0166 [33]		0.048 [31]

Table 2: Chemical composition of the Incoloy825 (mass percentage).

Al	Co	Cr	Cu	Mn	Mo	Ni	Si	Ti	Fe
0.096	0.44	20.62	1.95	0.46	3.1	41.74	0.336	1.01	Bal.

Table 3: Chemical composition of slag samples in each experimental heat (mass percentage).

Sample	CaO	SiO_2	Al_2O_3	MgO	Na_2O	CaF_2	Ce_2O_3
S0	30	30	15	5	10	10	0
S1	30	30	15	5	10	10	5
S2	30	30	15	5	10	10	10
S3	30	30	15	5	10	10	15
S4	30	30	15	5	10	10	20

indicating that the reactivity of both Al_2O_3 and SiO_2 in the mold flux is weakened.

This is because Ce_2O_3 is able to form compounds such as $CeAlO_3$ and $Ce_2Si_2O_7$ with Al_2O_3 and SiO_2, respectively [27, 28], reducing the activity of Al_2O_3 and SiO_2. In addition, when the content of Ce_2O_3 in the mold flux is 20%, a_{SiO_2} approaches 0.

2.2. Thermodynamic Analysis of Slag-Steel Reaction. In order to investigate the effect of adding Ce_2O_3 to mold flux on the slag-steel interfacial chemical reaction, $a_{Ce_2O_3}$, $a_{Al_2O_3}$, and a_{SiO_2} are calculated by IMCT and f_{Al}, f_{Si}, and f_{Ti} in steel were brought into Eq. (6), Eq. (9), and (2) to obtain the reaction Gibbs free energy of Eq. (4), Eq. (6), and Eq. (8). The composition of steel and mold fluxes is shown in Tables 2 and 3, respectively, and the calculation results are shown in Figure 3.

As shown in Figure 3, Ce_2O_3 component is added to the mold flux, and ΔG_1 is the minimum compared with ΔG_2 and ΔG_3. Therefore, the main slag-steel interfacial chemical reaction is $[Ti] + (SiO_2) = [Si] + (TiO_2)$, and the secondary reactions are the following: $4[Al] + 3(SiO_2) = 3[Si] + 2(Al_2O_3)$ and $3[Ti] + 2(Al_2O_3) = 4[Al] + 3(TiO_2)$. The reason is that a_{Ti} is much greater than a_{Al}, so Ti in steel is more susceptible to oxidation. With the increase of Ce_2O_3 content in mold flux, ΔG_1, ΔG_2, and ΔG_3 gradually increase, of which ΔG_1 increases the most. This is because Ce_2O_3 in the mold flux is combined with Al_2O_3 and SiO_2, which reduces the activities of Al_2O_3 and SiO_2 and weakens the slag-steel interfacial chemical reaction and inhibits the oxidation loss of Ti and Al in steel.

It can be seen from Figure 3 that CaO-SiO_2-Al_2O_3-based slag system will inevitably cause the oxidation of Al and Ti in steel, and the TiO_2 generated into the mold flux will lead to a change in the trend of each reaction. In order to better understand the trend of each reaction at the slag-steel interface, the influence of different TiO_2 contents on the slag-steel interfacial chemical reaction was calculated, where the calculation results of S0 slag system are shown in Figure 4.

As shown in Figure 4, when w(TiO_2) is less than 0.5%, ΔG_1 and ΔG_3 increase rapidly, and when w(TiO_2) is more than 0.5%, ΔG_1 and ΔG_3 increase slowly and gradually tend to equilibrium. This is due to the fact that TiO_2 generated by slag-steel interfacial chemical reaction causes a significant increase in the activity of TiO_2 and the interfacial chemical reactions of Eq. (4) and Eq. (8) are inhibited. However, there is no TiO_2 in the interfacial chemical reaction of Eq. (6), but with the increase of TiO_2 content in the mold flux, the mass percentage of Al_2O_3 and SiO_2 in the mold flux is changed, which makes Eq. (9) change to some extent, so ΔG_2 decreases slightly. When w(TiO_2) is 3%, at this time ΔG_3 is 0, the reaction Eq. (10) reaches an equilibrium state, and ΔG_1 and ΔG_2 are close. The slag-steel interfacial chemical reactions are the following: $[Ti] + (SiO_2) = [Si] + (TiO_2)$ and $4[Al] + 3(SiO_2) = 3[Si] + 2(Al_2O_3)$. However, when more TiO_2 components are added to the protective slag, TiO_2 will combine with CaO to form $CaTiO_3$. On the one hand, the actual activity of TiO_2 in the mold flux is small; on the other hand, the binding ability of CaO with Al_2O_3 and SiO_2 is reduced, which makes the activity of Al_2O_3 and SiO_2 increase, which is not conducive to reducing the oxidation of Al and Ti in steel.

3. Experiment and Results of Slag-Steel Reaction

3.1. Experimental Process. To simplify the desulfurization kinetic model, the following assumptions are needed: in order to further study the effect of the content of Ce_2O_3 in mold flux on the changes of Al, Si, and Ti contents of Incoloy825 alloy, the slag-steel experiments of Incoloy825 and mold flux with different Ce_2O_3 contents were carried out. The Incoloy825 used in the experiment was smelted in a 25 kg vacuum induction furnace, and the ingots were cut into small pieces by wire cutting. The surface of the sample

Table 4: Expression of structural units, their mole numbers, and mass action concentrations in 100 g CaO-SiO_2-Al_2O_3-Na_2O-MgO-CaF_2-Ce_2O_3 slags based on IMCT.

Item	Structural units (ion or molecule)	Mole number of structural units n_i	Mass action concentration of structural units N_i
Simple ion (5)	$Ca^{2+}+O^{2-}$	$n_{S1} = n_{Ca^{2+}} = n_{O^{2-}}$	$N_{S1} = N_{CaO} = 2n_{S1}/\sum n_i$
	$Na^{+}+O^{2-}$	$n_{S4} = 2n_{Na^{+}} = n_{O^{2-}}$	$N_{S4} = N_{Na_2O} = 3n_{S4}/\sum n_i$
	$Mg^{2+}+O^{2-}$	$n_{S5} = n_{Mg^{2+}} = n_{O^{2-}}$	$N_{S5} = N_{MgO} = 2n_{S5}/\sum n_i$
	$Ca^{2+}+2F^{-}$	$n_{S6} = n_{Ca^{2+}} = 2n_{F^{-}}$	$N_{S6} = N_{CaF_2} = 3n_{S6}/\sum n_i$
	$2Ce^{2+}+3O^{2-}$	$n_{S7} = 2n_{Ce^{3+}} = 3n_{O^{2-}}$	$N_{S7} = N_{Ce_2O_3} = 5n_{S7}/\sum n_i$
Simple molecule (2)	SiO_2	$n_{S2} = n_{SiO_2}$	$N_{S2} = N_{SiO_2} = n_{S2}/\sum n_i$
	Al_2O_3	$n_{S3} = n_{Al_2O_3}$	$N_{S3} = N_{Al_2O_3} = n_{S3}/\sum n_i$
Complex molecule (40)	$CaO \cdot SiO_2$	$n_{C1} = n_{CaO\cdot SiO_2}$	$N_{C1} = N_{CaO\cdot SiO_2} = n_{C1}/\sum n_i$
	$2CaO \cdot SiO_2$	$n_{C2} = n_{2CaO\cdot SiO_2}$	$N_{C2} = N_{2CaO\cdot SiO_2} = n_{C2}/\sum n_i$
	$3CaO \cdot SiO_2$	$n_{C3} = n_{3CaO\cdot SiO_2}$	$N_{C3} = N_{3CaO\cdot SiO_2} = n_{C3}/\sum n_i$
	$3CaO \cdot 2SiO_2$	$n_{C4} = n_{3CaO\cdot 2SiO_2}$	$N_{C4} = N_{3CaO\cdot 2SiO_2} = n_{C4}/\sum n_i$
	$CaO \cdot Al_2O_3$	$n_{C5} = n_{CaO\cdot Al_2O_3}$	$N_{C5} = N_{CaO\cdot Al_2O_3} = n_{C5}/\sum n_i$
	$CaO \cdot 2Al_2O_3$	$n_{C6} = n_{CaO\cdot 2Al_2O_3}$	$N_{C6} = N_{CaO\cdot 2Al_2O_3} = n_{C6}/\sum n_i$
	$CaO \cdot 6Al_2O_3$	$n_{C7} = n_{CaO\cdot 6Al_2O_3}$	$N_{C7} = N_{CaO\cdot 6Al_2O_3} = n_{C7}/\sum n_i$
	$3CaO \cdot Al_2O_3$	$n_{C8} = n_{3CaO\cdot Al_2O_3}$	$N_{C8} = N_{3CaO\cdot Al_2O_3} = n_{C8}/\sum n_i$
	$12CaO \cdot 7Al_2O_3$	$n_{C9} = n_{12CaO\cdot 7Al_2O_3}$	$N_{C9} = N_{12CaO\cdot 7Al_2O_3} = n_{C9}/\sum n_i$
	$3Al_2O_3 \cdot 2SiO_2$	$n_{C10} = n_{3Al_2O_3\cdot 2SiO_2}$	$N_{C10} = N_{3Al_2O_3\cdot 2SiO_2} = n_{C10}/\sum n_i$
	$Na_2O \cdot SiO_2$	$n_{C11} = n_{Na_2O\cdot SiO_2}$	$N_{C11} = N_{Na_2O\cdot SiO_2} = n_{C11}/\sum n_i$
	$Na_2O \cdot 2SiO_2$	$n_{C12} = n_{Na_2O\cdot 2SiO_2}$	$N_{C12} = N_{Na_2O\cdot 2SiO_2} = n_{C12}/\sum n_i$
	$2Na_2O \cdot SiO_2$	$n_{C13} = n_{2Na_2O\cdot SiO_2}$	$N_{C13} = N_{2Na_2O\cdot SiO_2} = n_{C13}/\sum n_i$
	$MgO \cdot SiO_2$	$n_{C14} = n_{MgO\cdot SiO_2}$	$N_{C14} = N_{MgO\cdot SiO_2} = n_{C14}/\sum n_i$
	$2MgO \cdot SiO_2$	$n_{C15} = n_{2MgO\cdot SiO_2}$	$N_{C15} = N_{2MgO\cdot SiO_2} = n_{C15}/\sum n_i$
	$Na_2O \cdot Al_2O_3$	$n_{C16} = n_{Na_2O\cdot Al_2O_3}$	$N_{C16} = N_{Na_2O\cdot Al_2O_3} = n_{C16}/\sum n_i$
	$Na_2O \cdot 3Al_2O_3$	$n_{C17} = n_{Na_2O\cdot 3Al_2O_3}$	$N_{C17} = N_{Na_2O\cdot 3Al_2O_3} = n_{C17}/\sum n_i$
	$Na_2O \cdot 9Al_2O_3$	$n_{C18} = n_{Na_2O\cdot 9Al_2O_3}$	$N_{C18} = N_{Na_2O\cdot 9Al_2O_3} = n_{C18}/\sum n_i$
	$MgO \cdot Al_2O_3$	$n_{C19} = n_{MgO\cdot Al_2O_3}$	$N_{C19} = N_{MgO\cdot Al_2O_3} = n_{C19}/\sum n_i$
	$Ce_2O_3 \cdot Al_2O_3$	$n_{C20} = n_{Ce_2O_3\cdot Al_2O_3}$	$N_{C20} = N_{Ce_2O_3\cdot Al_2O_3} = n_{C20}/\sum n_i$
	$Ce_2O_3 \cdot 11Al_2O_3$	$n_{C21} = n_{Ce_2O_3\cdot 11Al_2O_3}$	$N_{C21} = N_{Ce_2O_3\cdot 11Al_2O_3} = n_{C21}/\sum n_i$
	$CaO \cdot Al_2O_3 \cdot 2SiO_2$	$n_{C22} = n_{CaO\cdot Al_2O_3\cdot 2SiO_2}$	$N_{C22} = N_{CaO\cdot Al_2O_3\cdot 2SiO_2} = n_{C22}/\sum n_i$
	$2CaO \cdot Al_2O_3 \cdot 2SiO_2$	$n_{C23} = n_{2CaO\cdot Al_2O_3\cdot SiO_2}$	$N_{C23} = N_{2CaO\cdot Al_2O_3\cdot SiO_2} = n_{C23}/\sum n_i$
	$2Na_2O \cdot CaO \cdot 3SiO_2$	$n_{C24} = n_{2Na_2O\cdot CaO\cdot 3SiO_2}$	$N_{C24} = N_{2Na_2O\cdot CaO\cdot 3SiO_2} = n_{C24}/\sum n_i$
	$Na_2O \cdot CaO \cdot 5SiO_2$	$n_{C25} = n_{Na_2O\cdot CaO\cdot 5SiO_2}$	$N_{C25} = N_{Na_2O\cdot CaO\cdot 5SiO_2} = n_{C25}/\sum n_i$
	$Na_2O \cdot 2CaO \cdot 3SiO_2$	$n_{C26} = n_{Na_2O\cdot 2CaO\cdot 3SiO_2}$	$N_{C26} = N_{Na_2O\cdot 2CaO\cdot 3SiO_2} = n_{C26}/\sum n_i$
	$Na_2O \cdot 3CaO \cdot 6SiO_2$	$n_{C27} = n_{Na_2O\cdot 3CaO\cdot 6SiO_2}$	$N_{C27} = N_{Na_2O\cdot 3CaO\cdot 6SiO_2} = n_{C27}/\sum n_i$
	$CaO \cdot MgO \cdot SiO_2$	$n_{C28} = n_{CaO\cdot MgO\cdot SiO_2}$	$N_{C28} = N_{CaO\cdot MgO\cdot SiO_2} = n_{C28}/\sum n_i$
	$CaO \cdot MgO \cdot 2SiO_2$	$n_{C29} = n_{CaO\cdot MgO\cdot 2SiO_2}$	$N_{C29} = N_{CaO\cdot MgO\cdot 2SiO_2} = n_{C29}/\sum n_i$
	$2CaO \cdot MgO \cdot 2SiO_2$	$n_{C30} = n_{2CaO\cdot MgO\cdot 2SiO_2}$	$N_{C30} = N_{2CaO\cdot MgO\cdot 2SiO_2} = n_{C30}/\sum n_i$
	$3CaO \cdot MgO \cdot 2SiO_2$	$n_{C31} = n_{3CaO\cdot MgO\cdot 2SiO_2}$	$N_{C31} = N_{3CaO\cdot MgO\cdot 2SiO_2} = n_{C31}/\sum n_i$
	$3CaO \cdot 2SiO_2 \cdot CaF_2$	$n_{C32} = n_{3CaO\cdot 2SiO_2\cdot CaF_2}$	$N_{C32} = N_{3CaO\cdot 2SiO_2\cdot CaF_2} = n_{C32}/\sum n_i$
	$3CaO \cdot 3Al_2O_3 \cdot CaF_2$	$n_{C33} = n_{3CaO\cdot 2Al_2O_3\cdot CaF_2}$	$N_{C33} = N_{3CaO\cdot 2Al_2O_3\cdot CaF_2} = n_{C33}/\sum n_i$
	$11CaO \cdot 7Al_2O_3 \cdot CaF_2$	$n_{C34} = n_{11CaO\cdot 7Al_2O_3\cdot CaF_2}$	$N_{C34} = N_{11CaO\cdot 7Al_2O_3\cdot CaF_2} = n_{C34}/\sum n_i$
	$Na_2O \cdot Al_2O_3 \cdot 2SiO_2$	$n_{C35} = n_{Na_2O\cdot Al_2O_3\cdot 2SiO_2}$	$N_{C35} = N_{Na_2O\cdot Al_2O_3\cdot 2SiO_2} = n_{C35}/\sum n_i$
	$Na_2O \cdot Al_2O_3 \cdot 4SiO_2$	$n_{C36} = n_{Na_2O\cdot Al_2O_3\cdot 4SiO_2}$	$N_{C36} = N_{Na_2O\cdot Al_2O_3\cdot 4SiO_2} = n_{C36}/\sum n_i$
	$Na_2O \cdot Al_2O_3 \cdot 6SiO_2$	$n_{C37} = n_{Na_2O\cdot Al_2O_3\cdot 6SiO_2}$	$N_{C37} = N_{Na_2O\cdot Al_2O_3\cdot 6SiO_2} = n_{C37}/\sum n_i$
	$2MgO \cdot 2Al_2O_3 \cdot SiO_2$	$n_{C38} = n_{2MgO\cdot 2Al_2O_3\cdot SiO_2}$	$N_{C38} = N_{2MgO\cdot 2Al_2O_3\cdot SiO_2} = n_{C38}/\sum n_i$
	$Na_2O \cdot MgO \cdot 4SiO_2$	$n_{C39} = n_{Na_2O\cdot MgO\cdot 4SiO_2}$	$N_{C39} = N_{Na_2O\cdot MgO\cdot 4SiO_2} = n_{C39}/\sum n_i$
	$Na_2O \cdot 2MgO \cdot 6SiO_2$	$n_{C40} = n_{Na_2O\cdot 2MgO\cdot 6SiO_2}$	$N_{C40} = N_{Na_2O\cdot 2MgO\cdot 6SiO_2} = n_{C40}/\sum n_i$

Table 5: Chemical reaction formulas of possibly formed complex molecules.

Reaction	ΔG_i^θ (J/mol)	Reference	N_i
$(Ca^{2+} + O^{2-}) + (SiO_2) = (CaO \cdot SiO_2)$	$-21757 - 36.82T$	34	$N_{C1} = K_{C1}N_1N_2$
$2(Ca^{2+} + O^{2-}) + (SiO_2) = (2CaO \cdot SiO_2)$	$-102090 - 24.27T$	34	$N_{C2} = K_{C2}N_1^2N_2$
$3(Ca^{2+} + O^{2-}) + (SiO_2) = (3CaO \cdot SiO_2)$	$-118826 - 6.69T$	35	$N_{C3} = K_{C3}N_1^3N_2$
$3(Ca^{2+} + O^{2-}) + 2(SiO_2) = (3CaO \cdot 2SiO_2)$	$-236814 + 9.62T$	35	$N_{C4} = K_{C4}N_1^3N_2^2$
$(Ca^{2+} + O^{2-}) + (Al_2O_3) = (CaO \cdot Al_2O_3)$	$59413 - 59.41T$	34	$N_{C5} = K_{C5}N_1N_3$

Table 5: Continued.

Reaction	ΔG_i^θ (J/mol)	Reference	N_i
$(Ca^{2+} + O^{2-}) + 2(Al_2O_3) = (CaO \cdot 2Al_2O_3)$	$-16700 - 25.52T$	34	$N_{C6} = K_{C6}N_1N_3^2$
$(Ca^{2+} + O^{2-}) + 6(Al_2O_3) = (CaO \cdot 6Al_2O_3)$	$-22594 - 31.80T$	34	$N_{C7} = K_{C7}N_1N_3^6$
$3(Ca^{2+} + O^{2-}) + (Al_2O_3) = (3CaO \cdot Al_2O_3)$	$-21757 - 29.29T$	34	$N_{C8} = K_{C8}N_1^3N_3$
$12(Ca^{2+} + O^{2-}) + 7(Al_2O_3) = (12CaO \cdot 7Al_2O_3)$	$617977 - 612.12T$	34	$N_{C9} = K_{C9}N_1^{12}N_3^7$
$3(Al_2O_3) + 2(SiO_2) = (3Al_2O_3 \cdot 2SiO_2)$	$-4354 - 10.47T$	34	$N_{C10} = K_{C10}N_2^2N_3^3$
$(2Na^+ + O^{2-}) + (SiO_2) = (Na_2O \cdot SiO_2)$	$-299349 + 55.32T$	36	$N_{C11} = K_{C11}N_2N_4$
$(2Na^+ + O^{2-}) + 2(SiO_2) = (Na_2O \cdot 2SiO_2)$	$-279094 + 23.19T$	36	$N_{C12} = K_{C12}N_2^2N_4$
$2(2Na^+ + O^{2-}) + (SiO_2) = (2Na_2O \cdot SiO_2)$	$-517220 + 124.22T$	36	$N_{C13} = K_{C13}N_2N_4^2$
$(Mg^{2+} + O^{2-}) + (SiO_2) = (MgO \cdot SiO_2)$	$23849 - 29.71T$	34	$N_{C14} = K_{C14}N_2N_5$
$2(Mg^{2+} + O^{2-}) + (SiO_2 = (2MgO \cdot SiO_2)$	$-56902 - 3.35T$	34	$N_{C15} = K_{C15}N_2N_5^2$
$(2Na^+ + O^{2-}) + (Al_2O_3) = (Na_2O \cdot Al_2O_3)$	$-247971 + 44.6T$	36	$N_{C16} = K_{C16}N_3N_4$
$(2Na^+ + O^{2-}) + 3(Al_2O_3) = (Na_2O \cdot 3Al_2O_3)$	$-282626 + 35.28T$	36	$N_{C17} = K_{C17}N_3^3N_4$
$(2Na^+ + O^{2-}) + 9(Al_2O_3) = (Na_2O \cdot 9Al_2O_3)$	$-295918 + 25.18T$	36	$N_{C18} = K_{C18}N_3^9N_4$
$(Mg^{2+} + O^{2-}) + (Al_2O_3) = (MgO \cdot Al_2O_3)$	$-18828 - 6.28T$	34	$N_{C19} = K_{C19}N_3N_5$
$(2Ce^{3+} + 3O^{2-}) + (Al_2O_3) = (Ce_2O_3 \cdot Al_2O_3)$	$-60241 - 14.19T$	37	$N_{C20} = K_{C20}N_3N_7$
$(2Ce^{3+} + 3O^{2-}) + 11(Al_2O_3) = (Ce_2O_3 \cdot 11Al_2O_3)$	$49332 - 80.56T$	37	$N_{C21} = K_{C21}N_3^{11}N_7$
$(Ca^{2+} + O^{2-}) + (Al_2O_3) + 2(SiO_2) = (CaO \cdot Al_2O_3 \cdot 2SiO_2)$	$-13816 - 55.26T$	36	$N_{C22} = K_{C22}N_1N_2^2N_3$
$2(Ca^{2+} + O^{2-}) + (Al_2O_3) + (SiO_2) = (2CaO \cdot Al_2O_3 \cdot SiO_2)$	$-61961 - 60.29T$	36	$N_{C23} = K_{C23}N_1^2N_2N_3$
$2(2Na^+ + O^{2-}) + (Ca^{2+} + O^{2-}) + 3(SiO_2) = (Na_2O \cdot CaO \cdot 3SiO_2)$	$-672020 + 62.8\,T$	36	$N_{C24} = K_{C24}N_1N_2^3N_4^2$
$(2Na^+ + O^{2-}) + (Ca^{2+} + O^{2-}) + 5(SiO_2) = (Na_2O \cdot CaO \cdot 5SiO_2)$	$-443841 + 63.84T$	36	$N_{C25} = K_{C25}N_1N_2^5N_4$
$(2Na^+ + O^{2-}) + 2(Ca^{2+} + O^{2-}) + 3(SiO_2) = (Na_2O \cdot 2CaO \cdot 3SiO_2)$	$-607293 + 125.68T$	36	$N_{C26} = K_{C26}N_1^2N_2^3N_4$
$(2Na^+ + O^{2-}) + 3(Ca^{2+} + O^{2-}) + 6(SiO_2) = (Na_2O \cdot 3CaO \cdot 6SiO_2)$	$-837543 + 219.7T$	36	$N_{C27} = K_{C27}N_1^3N_2^6N_4$
$(Ca^{2+} + O^{2-}) + (Mg^{2+} + O^{2-}) + (SiO_2) = (CaO \cdot MgO \cdot SiO_2)$	$-124683 + 0.77T$	35	$N_{C28} = K_{C28}N_1N_2N_5$
$(Ca^{2+} + O^{2-}) + (Mg^{2+} + O^{2-}) + 2(SiO_2) = (CaO \cdot MgO \cdot 2SiO_2)$	$-80{-}51.88T$	34	$N_{C29} = K_{C29}N_1N_2^2N_5$
$2(Ca^{2+} + O^{2-}) + (Mg^{2+} + O^{2-}) + 2(SiO_2) = (2CaO \cdot MgO \cdot 2SiO_2)$	$-73638 - 63.29T$	34	$N_{C30} = K_{C30}N_1^2N_2^2N_5$
$3(Ca^{2+} + O^{2-}) + (Mg^{2+} + O^{2-}) + 2(SiO_2) = (3CaO \cdot MgO \cdot 2SiO_2)$	$-205016 - 31.80T$	34	$N_{C31} = K_{C31}N_1^3N_2^2N_5$
$3(Ca^{2+} + O^{2-}) + 2(SiO_2) + (Ca^{2+} + 2F^-) = (3CaO \cdot 2SiO_2 \cdot CaF_2)$	$-255180 - 8.2T$	34	$N_{C32} = K_{C32}N_1^3N_2^2N_6$
$3(Ca^{2+} + O^{2-}) + 3(Al_2O_3) + (Ca^{2+} + 2F^-) = (3CaO \cdot 3Al_2O_3 \cdot CaF_2)$	$-44492 - 73.15T$	38	$N_{C33} = K_{C33}N_1^3N_3^3N_6$
$11(Ca^{2+} + O^{2-}) + 7(Al_2O_3) + (Ca^{2+} + 2F^-) = (11CaO \cdot 7Al_2O_3 \cdot CaF_2)$	$-228760 - 155.8T$	38	$N_{C34} = K_{C34}N_1^{11}N_3^7N_6$
$(2Na^+ + O^{2-}) + (Al_2O_3) + 2(SiO_2) = (Na_2O \cdot Al_2O_3 \cdot 2SiO_2)$	$-370572.02 + 9.98T$	36	$N_{C35} = K_{C35}N_2^2N_3N_4$
$(2Na^+ + O^{2-}) + (Al_2O_3) + 4(SiO_2) = (Na_2O \cdot Al_2O_3 \cdot 4SiO_2)$	$-440860 + 101.36T$	36	$N_{C36} = K_{C36}N_2^4N_3N_4$
$(2Na^+ + O^{2-}) + (Al_2O_3) + 6(SiO_2) = (Na_2O \cdot Al_2O_3 \cdot 6SiO_2)$	$-425604 + 19.38T$	36	$N_{C37} = K_{C37}N_2^6N_3N_4$
$2(Mg^{2+} + O^{2-}) + 2(Al_2O_3) + 5(SiO_2) = (2MgO \cdot 2Al_2O_3 \cdot 5SiO_2)$	$-14422 - 14.81T$	34	$N_{C38} = K_{C38}N_2^5N_3^2N_5^2$
$(2Na^+ + O^{2-}) + (Mg^{2+} + O^{2-}) + 4(SiO_2) = (Na_2O \cdot MgO \cdot 4SiO_2)$	$-306210 - 1.2T$	36	$N_{C39} = K_{C39}N_2^4N_4N_5$
$(2Na^+ + O^{2-}) + 2(Mg^{2+} + O^{2-}) + 6(SiO_2) = (Na_2O \cdot 2MgO \cdot 6SiO_2)$	$-312061 - 33.06T$	36	$N_{C40} = K_{C40}N_2^6N_4N_5^2$

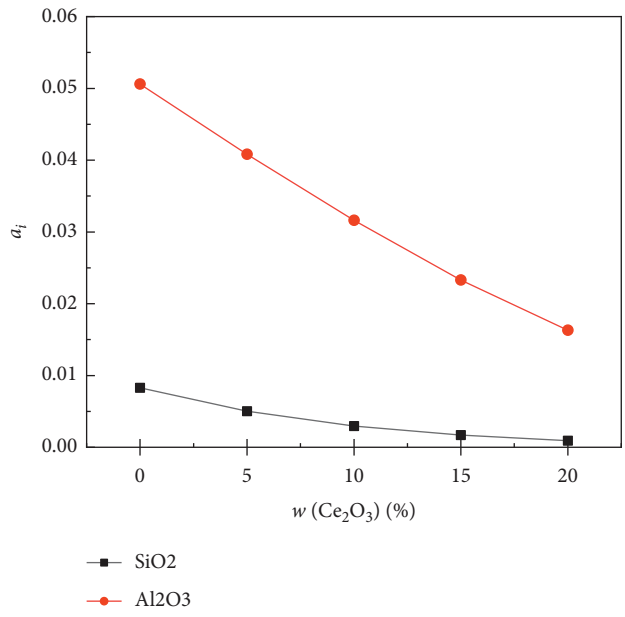

Figure 2: Influence of (w) (Ce_2O_3) on the activity of Al_2O_3 and SiO_2.

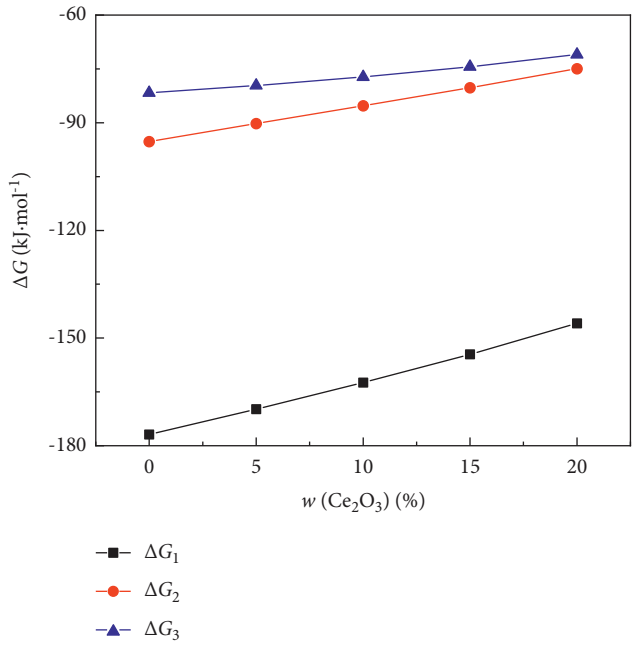

Figure 3: Gibbs free energy of the slag-steel interface chemical reaction with different Ce_2O_3 contents.

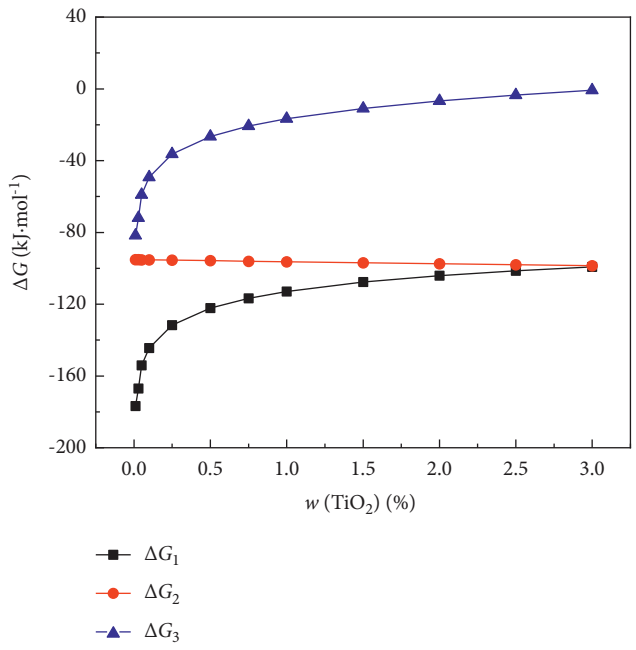

Figure 4: Gibbs free energy of the slag-steel interface chemical reaction with different TiO_2 contents for S0.

was angularly ground to remove the oxide from its surface to ensure the accuracy of the experiment. The compositions are shown in Table 2.

According to Figure 1(c), the $CaO\text{-}SiO_2\text{-}Al_2O_3$-based mold fluxes were designed, and the appropriate fluxes were added. Using analytical grade CaO, SiO_2, Al_2O_3, MgO, Na_2CO_3 (instead of Na_2O), CaF_2, and $Ce_2C_3O_9$ (instead of Ce_2O_3) as raw materials (purity >99%), CaO, MgO, and

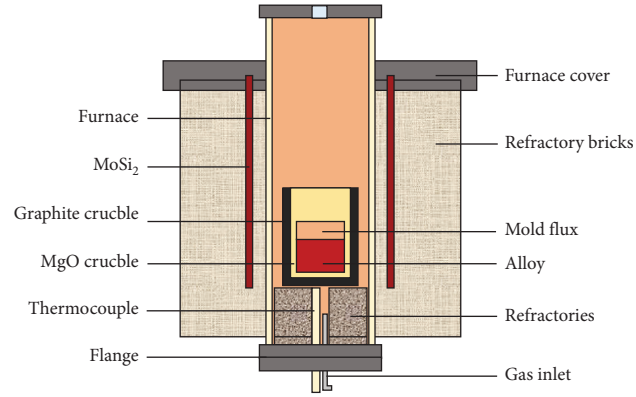

Figure 5: Schematic diagram of the experimental resistance furnace.

$Ce_2C_3O_9$ powders were calcined in a muffle furnace at 873 K for 2 h to remove moisture. The chemical compositions of mold flux used in the experiment are shown in Table 3.

A vertical $MoSi_2$ resistance furnace was used to carry out slag-steel reaction equilibrium experiment. The schematic diagram of the experimental device used is shown in Figure 5. The furnace body is made of corundum tubes with an inner diameter of 90 mm and a length of 1000 mm. The temperature of the furnace is measured by a B thermocouple (Pt-30% Rh/Pt-6% Rh), and the temperature deviation can be kept within 2 K in the temperature uniform zone (100 mm).

The experimental process is as follows: first, 500 g of treated Incoloy825 was put into MgO-crucible, which was covered with graphite crucible, and then put into a $MoSi_2$ resistance furnace, and argon (purity is 99%) was introduced at a flow rate of 1 L/min. Then, the temperature of the resistance furnace was raised to 1693 K at 5 K/min, and the constant temperature was maintained for about 30 mins to ensure the complete melting of the alloy in the furnace. Appropriately increased argon flow rate to ensure the atmosphere environment in the furnace during sampling, and the molten steel was sucked by a quartz tube with an inner diameter of 6 mm and recorded as 0 #. Finally, 100 g slag was added to the surface of the molten metal. After the slag was melted for 10, 20, 30, and 40 minutes, respectively, samples 1 # to 4 # were extracted from the molten metal, and a certain amount of slag samples was dipped at the same time. The cooled steel samples and slag samples were put into sample bags and marked with serial numbers.

3.2. Experimental Results and Discussion. Figure 6 shows the changes of Al, Si, and Ti in Incoloy825 with time during the experiment. The mold fluxes with different Ce_2O_3 contents have great influence on the contents of Al, Si, and Ti in Incoloy825. As shown in Figures 6(a)-6(d), the Al content is basically unchanged for 20 mins before the reaction and slightly increases for 20 mins to 40 mins after the reaction. The change of Al content in S4 slag system is most obvious,

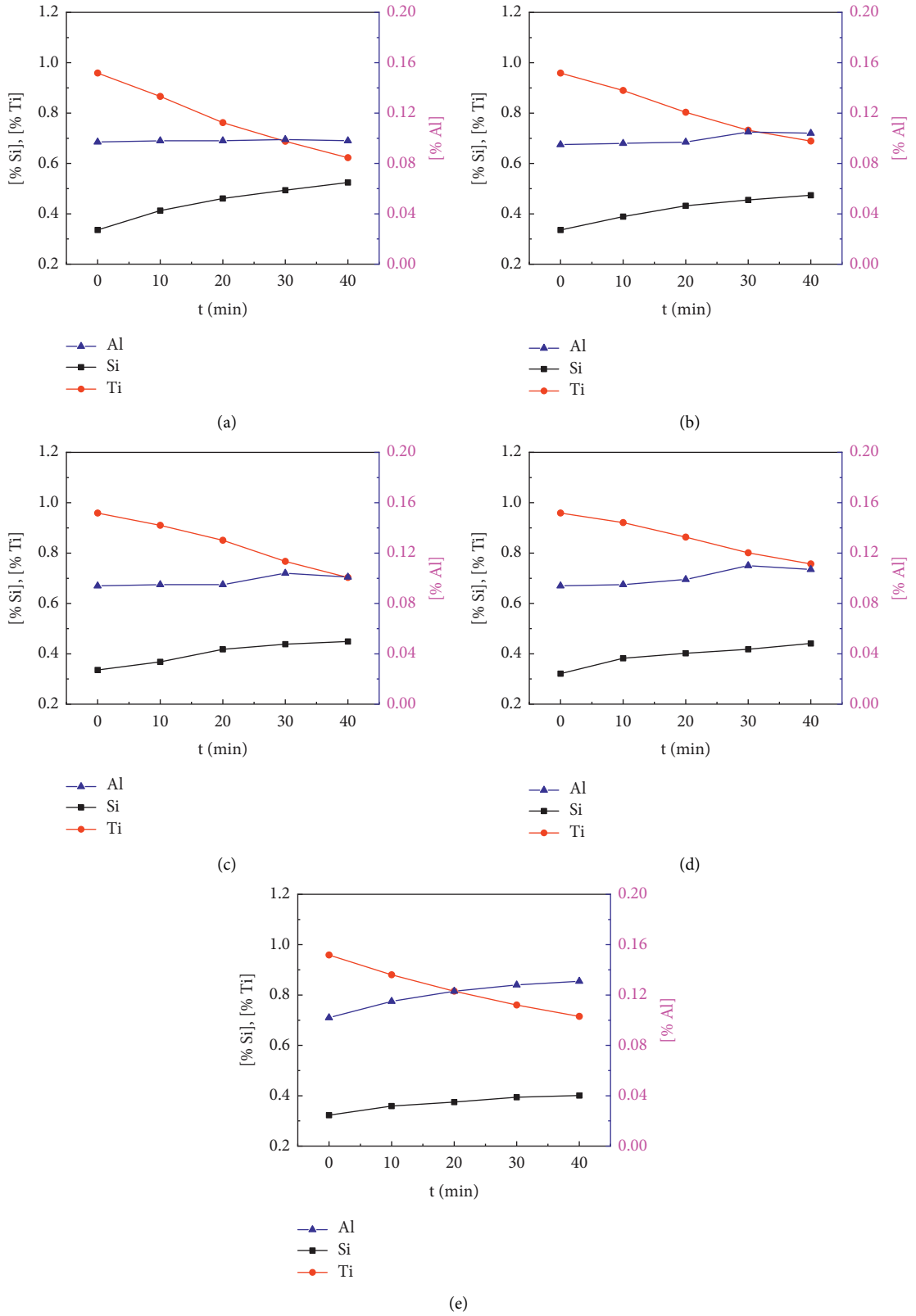

Figure 6: Changes of Al, Si, and Ti contents with time in Incoloy825: (a) S0, (b) S1, (c) S2, (d) S3, and (e) S4.

as shown in Figure 6(e), and the increase rate of Al content in steel is from 1.03% to 35.05%. Eq. (6) and Eq. (8) are carried out synchronously, where the content of Al maintains a dynamic equilibrium. As the activity of SiO_2 decreases, the reactivity of Eq. (6) becomes weaker, so the concentration of Al increased with time.

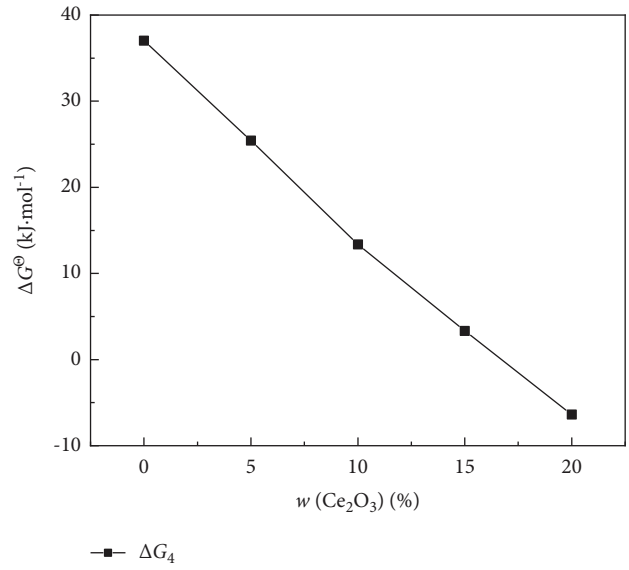

Figure 7: Gibbs free energy of the slag-steel interface chemical reaction with different Ce_2O_3 contents.

It can be seen from Figures 6(a)-6(e) that with the increase of slag-steel interfacial chemical reaction time, the content of Si in steel gradually increases and the content of Ti gradually decreases. The increase rate of Si content is from 55.95% to 19.35%, and the decrease rate of Ti content is from 33.27% to 20.00% when the increase of Ce_2O_3 content in the mold flux and the slag-steel reaction for 40 mins. The minimum oxidation loss of Ti appeared in slag S3 because the activity of Ti in steel will reduce the stable Ce_2O_3 in the mold flux, as shown in Eq. (13). The $a_{Ce_2O_3}$ and Ce contents in IMCT are brought into (14), and the calculated results are shown in Figure 7.

$$3[\mathrm{Ti}] + 2(\mathrm{Ce_2O_3}) = 4[\mathrm{Ce}] + 3(\mathrm{TiO_2}), \tag{13}$$

$$\begin{aligned} \Delta G_4^{\theta} &= 755431.34 - 188.79T, \\ \Delta G_4 = \Delta G_4^{\theta} + RT\ln K_4 &= \Delta G_4^{\theta} + RT\ln\frac{a_{\mathrm{Ce}}^4 \cdot a_{\mathrm{TiO_2}}^3}{a_{\mathrm{Ti}}^3 \cdot a_{\mathrm{Ce_2O_3}}^2} \\ &= \Delta G_3^{\theta} + RT\ln\frac{f_{\mathrm{Ce}}^4 \cdot w[\mathrm{Ce}]_{\%}^4}{f_{\mathrm{Ti}}^3 \cdot w[\mathrm{Ti}]_{\%}^3} + RT\ln\frac{a_{\mathrm{TiO_2}}^3}{a_{\mathrm{Ce_2O_3}}^2}. \end{aligned} \tag{14}$$

With the increase of Ce_2O_3 content in mold flux, ΔG_4 decreases gradually. When w(Ce_2O_3) is more than 15%, ΔG_4 is less than 0. At this time, Eq. (13) has a chemical reaction at the slag-steel interface. The reaction will lead to the oxidation of Ti and decrease the content of Ti in steel, so the content of Ce_2O_3 in mold flux should be less than 15%.

4. Conclusions

The effect of mold flux containing Ce_2O_3 on the contents of aluminum, silicon, and titanium in Incoloy825 super alloy was studied. The results are as follows:

(1) The activity model of CaO-SiO_2-Al_2O_3-Na_2O-MgO-CaF_2-Ce_2O_3 slag system was established based on the ion and molecule coexistence theory. The calculation results show that with the increase of Ce_2O_3 content in the mold flux, the activity of Al_2O_3 decreases significantly and the activity of SiO_2 decreases and gradually tends to 0.

(2) In the present study system, the main slag-steel interfacial chemical reaction is as follows: [Ti] + (SiO_2) = [Si] + (TiO_2), and the secondary reactions are as follows: 4[Al] + 3(SiO_2) = 3[Si] + 2(Al_2O_3) and 3 [Ti] + 2(Al_2O_3) = 4[Al] + 3(TiO_2).

(3) The results of slag-steel reaction experiment show that the increase rate of Al content increases from 1.03% to 10.31%, the increase rate of Si content decreases from 55.95% to 31.25%, and the oxidation rate of Ti content decreases from 33.27% to 20.00% when Ce_2O_3 content in the mold flux increases from 0% to 15% and the slag-steel reaction for 40 mins.

(4) With the increase of Ce_2O_3 content in the mold flux, the slag-steel interfacial chemical reaction is weakened, and the oxidation loss of Ti and Al in steel is inhibited. When the content of Ce_2O_3 in mold flux is more than 15%, the following chemical reaction will occur at the slag-steel interface: 3[Ti] +2(Ce_2O_3) = 4 [Ce] +3(TiO_2), which will aggravate the oxidation loss of Ti in steel, so the content of Ce_2O_3 in the mold flux should be less than 15% [36–38].

Data Availability

https://sycs.neu.edu.cn/.

Conflicts of Interest

The authors declare that there are no conflicts of interest.

Acknowledgments

This work was supported by the National Natural Science Foundation of China (U1760206).

References

[1] H. Singh, D. Puri, and S. Prakash, "Studies of plasma spray coatings on a Fe-base superalloy, their structure and high temperature oxidation behaviour," *Anti-corrosion Methods & Materials*, vol. 52, no. 2, pp. 84–95, 2005.

[2] S. Prabhu and B. K. Vinayagam, "AFM nano analysis of inconel 825 with single wall carbon nano tube in die sinking EDM process using taguchi analysis," *Arabian Journal for Science and Engineering*, vol. 38, no. 6, pp. 1599–1613, 2013.

[3] X. Xing, X. Di, and B. Wang, "The effect of post-weld heat treatment temperature on the microstructure of Inconel 625 deposited metal," *Journal of Alloys and Compounds*, vol. 593, pp. 110–116, 2014.

[4] H. Aytekin and Y. Akcin, "Characterization of borided Incoloy 825 alloy," *Materials & Design*, vol. 50, pp. 515–521, 2013.

[5] T. Feyzi and S. M. Safavi, "Improving machinability of Inconel 718 with a new hybrid machining technique," *Int. The International Journal of Advanced Manufacturing Technology*, vol. 66, pp. 1025–1030, 2012.

[6] S. K. Tamang and M. Chandrasekaran, "Integrated optimization methodology for intelligent machining of inconel 825 and its shop-floor application," *Journal of the Brazilian Society of Mechanical Sciences and Engineering*, vol. 39, pp. 865–877, 2017.

[7] J. D. Busch, J. J. Debarbadillo, and M. J. M. Krane, "Flux entrapment and titanium nitride defects in electroslag remelting of INCOLOY alloys 800 and 825," *Metallurgical and Materials Transactions A*, vol. 44, no. 12, pp. 5295–5303, 2013.

[8] Z. H. Jiang, D. Hou, Y. W. Dong, Y. L. Cao, H. B. Cao, and W. Gong, "Effect of Slag on Titanium, Silicon, and Aluminum Contents in Superalloy During Electroslag Remelting," *Metallurgical and Materials Transactions B*, vol. 47, pp. 1465–1474, 2016.

[9] W. Zhen, Q. F. Shu, and K. Chou, "Crystallization Kinetics and Structure of Mold Fluxes with SiO_2 Being Substituted by TiO_2 for Casting of Titanium-Stabilized Stainless Steel," *Metallurgical and Materials Transactions B*, vol. 44, pp. 606–613, 2013.

[10] J. Y. Li, G. G. Cheng, Q. Ruan, J. X. Pan, and X. Chen, "Characteristics of nozzle clogging and evolution of oxide inclusion for Al-killed Ti-stabilized 18Cr stainless steel," *Metallurgical and Materials Transactions B*, vol. 50, no. 6, pp. 2769–2779, 2019.

[11] C. B. Shi, M. D. Seo, J. W. Cho, and S. H. Kim, "Crystallization Characteristics of CaO-Al2O3-Based Mold Flux and Their Effects on In-Mold Performance during High-Aluminum TRIP Steels Continuous Casting," *Metallurgical and Materials Transactions B*, vol. 45, pp. 1081–1097, 2014.

[12] C. X. Ji, Y. Cui, Z. Zeng, Z. H. Tian, C. L. Zhao, and G. S. Zhu, "Continuous Casting of High-Al Steel in Shougang Jingtang Steel Works," *Journal of Iron and Steel Research International*, vol. 22, pp. 53–56, 2015.

[13] J. Qi, C. J. Liu, D. P. Yang, C. Zhang, and M. F. Jiang, "Study of a New Mold Flux for Heat-Resistant Steel Containing Cerium Continuous Casting," *Steel Research International*, vol. 87, pp. 890–898, 2016.

[14] J. W. Cho, K. Blazek, M. Frazee, H. B. Yin, J. H. Park, and S. W. Moon, "Assessment of CaO-Al2O3 Based Mold Flux System for High Aluminum TRIP Casting," *ISIJ International*, vol. 53, pp. 62–70, 2013.

[15] L. Zhang, B. Y. Zhai, W. L. Wang, and I. Sohn, "Effects of (CaO+BaO)/Al2O3 Ratio on the Melting, Crystallization, and Melt Structure of CaO-Al2O3-10wt%SiO2-Based Mold Fluxes for Advanced High-Strength Steels," *Journal of Sustainable Metallurgy*, vol. 7, pp. 559–568, 2021.

[16] S. P. He, Z. R. Li, Z. Chen, T. Wu, and Q. Wang, "Review of Mold Fluxes for Continuous Casting of High-Alloy (Al, Mn, Ti) Steels," *Steel Research International*, vol. 90, Article ID 1800424, 2019.

[17] L. J. Zhou, H. F. Wu, W. L. Wang, H. Luo, and H. Li, "Crystallization behavior and melt structure of typical CaO-SiO_2 and CaO-Al_2O_3-Based mold fluxes," *Ceramics International*, vol. 47, no. 8, pp. 10940–10949, 2020.

[18] B. Lu, K. Chen, W. Wang, and B. Jiang, "Effects of Li_2O and Na_2O on the crystallization behavior of lime-alumina-based mold flux for casting high-Al steels," *Metallurgical and Materials Transactions B*, vol. 45, no. 4, pp. 1496–1509, 2014.

[19] W. Wang, B. Lu, and D. Xiao, "A Review of Mold Flux Development for the Casting of High-Al Steels," *Metallurgical and Materials Transactions B*, vol. 47, pp. 384–389, 2016.

[20] Z. L. Piao, L. G. Zhu, X. J. Wang et al., "Effects of BaO on the viscosity and structure of a new fluorine-free CaO-Al_2O_3-TiO_2-based mold flux for high titanium steel," *Metallurgical and Materials Transactions B*, vol. 51, no. 5, pp. 2119–2130, 2020.

[21] D. Hou, Z. H. Jiang, Y. W. Dong, Y. L. Cao, H. B. Cao, and W. Gong, "Thermodynamic design of electroslag remelting slag for high titanium and low aluminium stainless steel based on IMCT," *Ironmaking and Steelmaking*, vol. 43, no. 7, pp. 517–525, 2016.

[22] D. Hou, P. Pan, D. Wang, S. Hu, H. Wang, and G. Zhang, "Study on the Melting Temperature of CaF2-CaO-MgO-Al2O3-TiO2 Slag under the Condition of a Fixed Ratio of Titanium and Aluminum in the Steel during the Electroslag Remelting Process," *Materials*, vol. 14, pp. 6047–6056, 2021.

[23] J. L. Li, Q. F. Shu, X. M. Hou, and K. C. Chou, "Effect of TiO_2 addition on crystallization characteristics of CaO-Al_2O_3-based mould fluxes for high Al steel casting," *ISIJ International*, vol. 55, no. 4, pp. 830–836, 2015.

[24] J. L. Li, Q. F. Shu, and K. C. Chou, "Effect of TiO_2 addition on viscosity and structure of CaO-Al_2O_3 based mould fluxes for high Al steel casting," *Canadian Metallurgical Quarterly*, vol. 54, no. 1, pp. 85–91, 2015.

[25] K. Zheng, Z. T. Zhang, L. L. Liu, and X. D. Wang, "Investigation of the viscosity and structural properties of CaO-SiO_2-TiO_2 slags," *Metallurgical and Materials Transactions B*, vol. 45, no. 4, pp. 1389–1397, 2014.

[26] H. Nakada and K. Nagata, "Crystallization of CaO-SiO_2-TiO_2 slag as a candidate for fluorine free mold flux," *ISIJ International*, vol. 46, no. 3, pp. 441–449, 2006.

[27] A. C. Tas and M. Akinc, "Phase Relations in the System Ce2O3-Ce2Si2O7 in the Temperature Range 1150° to 1970°C in Reducing and Inert Atmospheres," *Journal of the American Ceramic Society*, vol. 77, pp. 2953–2960, 1994.

[28] A. C. Tas and M. Akinc, "Phase Relations in the System Ce2O3-Al2O3 in Inert and Reducing Atmospheres," *Journal of the American Ceramic Society*, vol. 77, pp. 2961–2967, 1994.

[29] W. Jerzak and Z. Kalicka, "Evolution of equilibrium composition of MnO-SiO2 and Al2O3-MnO-SiO2 inclusions in liquid Fe and Fe-36%Ni alloy during cooling," *Archives of Metallurgy and Materials*, vol. 57, pp. 449–455, 2012.

[30] A. Karasev and H. Suito, "Quantitative evaluation of inclusion in deoxidation of Fe-10 mass pct Ni alloy with Si, Ti, Al, Zr, and Ce," *Metallurgical and Materials Transactions B*, vol. 30, no. 2, pp. 249–257, 1999.

[31] J. J. Pak, Y. S. Jeong, S. J. Tae, D. S. Kim, and Y. Y. Lee, "Thermodynamics of titanium and nitrogen in an Fe-Ni melt," *Metallurgical and Materials Transactions B*, vol. 36, no. 4, pp. 489–493, 2005.

[32] K. Suzuki, S. Ban-Ya, and M. Hino, "Deoxidation equilibrium of Cr-Ni stainless steel with Si at the temperatures from 1823 to 1923 K," *ISIJ International*, vol. 42, no. 2, pp. 146–149, 2002.

[33] T. Yoshikawa and K. Morita, "Influence of alloying elements on the thermodynamic properties of titanium in molten steel," *Metallurgical and Materials Transactions B*, vol. 38, no. 4, pp. 671–680, 2007.

[34] X. M. Yang, C. B. Shi, M. Zhang, J. P. Duan, and J. Zhnag, "Thermodynamic Model of Phosphate Capacity for CaO-SiO2-MgO-FeO-Fe2O3-MnO-Al2O3-P2O5 Slags Equilibrated with Molten Steel during a Top-Bottom Combined Blown Converter Steelmaking Process Based on the Ion and

Molecule Coexistence Theory," *Metallurgical and Materials Transactions B*, vol. 42, pp. 951–977, 2011.

[35] X. M. Yang, J. P. Duan, C. B. Shi, M. Zhang, Y. L. Zhang, and J. C. Wang, "A thermodynamic model of phosphorus distribution ratio between $CaO\text{-}SiO_2\text{-}MgO\text{-}FeO\text{-}Fe_2O_3\text{-}MnO\text{-}Al_2O_3\text{-}P_2O_5$ slags and molten steel during a top-bottom combined blown converter steelmaking process based on the ion and molecule coexistence theory," *Metallurgical and Materials Transactions B*, vol. 42, no. 4, pp. 738–770, 2011.

[36] J. L. Lei, D. N. Zhao, and H. Y. Zhu, "A thermodynamic model of desulfurization for CaO-SiO2-MgO-Al2O3-Na2O slag based on IMCT theory," *Iron and Steel*, vol. 54, no. 03, pp. 35–41, 2019.

[37] J. Qi, *Design and Basic Properties Investigation of Mold Fluxes for Rare Earth-Bearing Heat-Resistant Steel Continuous Casting [D]*, Northeastern University, Shenyang, 2018.

[38] D. Hou, Z. H. Jiang, Y. W. Dong, W. Gong, Y. L. Cao, and H. B. Cao, "Effect of slag composition on the oxidation kinetics of alloying elements during electroslag remelting of stainless steel: Part-1 mass-transfer model," *ISIJ International*, vol. 57, no. 8, pp. 1400–1409, 2017.